DESIGN OF LOW LEVEL RF CONTROL FOR THE TESLA SUPERSTRUCTURE

S. Michizono †, KEK, Tsukuba, Japan
M. Liepe, S. N. Simrock, DESY, Hamburg, Germany

Abstract

The superstructure is a viable option for the TESLA linear collider because of a high effective gradient and a reduced number of rf components. However, the high number and close proximity of passband modes impose challenging demands on the rf control system. The control problem is complicated by the fact that the cavity probe signal does not exactly reflect the actual accelerating voltage experienced by the beam due to the different coupling of the generator, pickup probe and beam to the FM passband modes. The digital control system developed for the standard 9-cell cavity is not adequate for operation of the superstructure. As discussed in this paper, an additional filter is needed to guarantee robustness and stability. Based on rf control simulations the filter characteristic is optimized.

1 INTRODUCTION

The performance of the superstructure [1] is planned to be tested with beam at the TESLA test facility (TTF). The main advantages of using superstructures are their higher space efficiency and fewer rf components. However, the superstructure (4x7-cell cavity) has 28 modes (fundamental acceleration mode is 25th mode). Since the nearest mode (26th) is located only about 150 kHz above the operation frequency (1.3 GHz), careful LLRF control is important.

In the TTF LLRF system, the down-converter (250 kHz) is used to detect the Inphase (I) and Quadrature (Q) components of the cavity field [2]. The signal obtained every 1 μs corresponds to one of I, Q -I and -Q. In order to reduce the excitation of the 26th mode, a bandpass filter (BPF) with the center frequency of 250 kHz (the carrier frequency) is inevitable for stable operation. The amplitude and phase errors are required to be less than 0.5% and 0.5 degree, respectively [3].

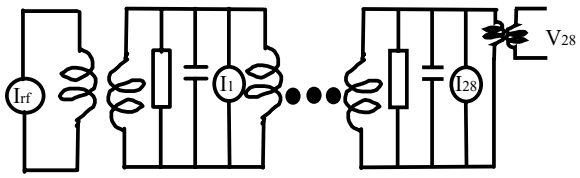

Figure 1 Schematic of the cavity model by a LCR circuit. Each cell couples with the adjacent cell. I_{rf} represents the generator drive while I_1,…I_{28} describe excitation of the individual cells by the beam.

†michizon@almond.kek.jp

2 BASIC EQUATIONS FOR LLRF

The calibrated cavity probe voltage (V_{probe}) is measured through a coupler adjacent to the 28th cell (last cell), as schematically shown in Figure 1. In the following the calibrations are such that $V_{probe}(25)$ equals the beam-acceleration voltage $V_{acc}(25)$ for the 25th mode (accelerating mode). Although the electron beam (I_b) excites the modes slightly (except 25th mode), the rf source (I_{rf}) having about 20 MHz bandwidth [2] can excite all of the modes.

The different couplings of the generator and the beam to the 28 passband modes are described by r/q(n) and R/Q(n) respectively. The cavity excitation is given by:

$$\ddot{V}_{probe} + \frac{\omega_0}{Q_l}\dot{V}_{probe} + {\omega_0}^2 V_{probe} = \frac{\omega_0}{2}\frac{r}{q}\dot{I}_{rf} - \frac{\omega_0}{2}\frac{R}{Q}\dot{I}_b \quad . \quad (1)$$

Suppose that the stored energy of each mode is unity,

$$U(n) = 1 = \frac{v^2_{probe}(n)}{\omega_0(n)\frac{r}{q}(n)} = \frac{v^2_{probe}(25)}{\omega_0(25)\frac{R}{Q}(25)} \quad . \quad (2)$$

Thus, the r/q is written as

$$\frac{r}{q}(n) = \frac{\omega_0(25)}{\omega_0(n)}\frac{v^2_{probe}(n)}{v^2_{probe}(25)}\frac{R}{Q}(25) \ , \quad (3)$$

where $v_{probe}(n)$ and $v_{probe}(25)$ are the "unit" cavity probe voltage corresponding to the unity energy of the nth and 25th modes, respectively.

By introducing the 'unit' beam acceleration voltage (v_{acc}) corresponding to the unit stored energy,

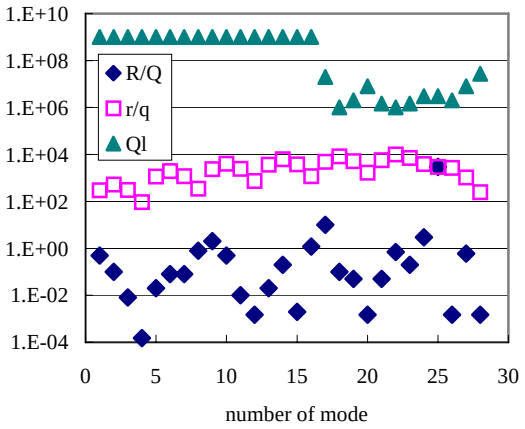

Figure 2 r/q distribution of each mode. R/Q and Q_l are referred from [1].

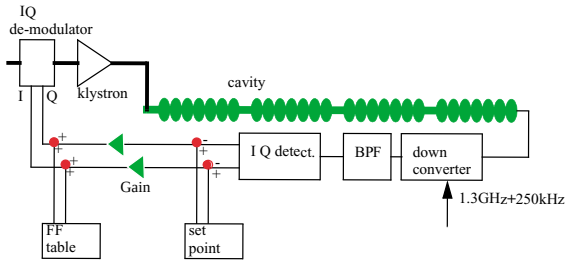

Figure 3 Schematic of the rf system. The pick-up signal of the cavity probe voltage is down-converted to 250 kHz. A bandpass filter is used for reducing the adjacent 26th mode.

$$U(n)=1=\frac{v^2_{probe}(n)}{\omega_0(n)\frac{r}{q}(n)}=\frac{v^2_{acc}(n)}{\omega_0(n)\frac{R}{Q}(n)} \quad . \quad (4)$$

Thus, the relation between the beam-acceleration voltage and the probe voltage is expressed as

$$\frac{V_{acc}(n)}{V_{probe}(n)}=\sqrt{\frac{\frac{R}{Q}(n)}{\frac{r}{q}(n)}}=\sqrt{\frac{\omega_0(n)\frac{R}{Q}(n)}{\omega_0(25)\frac{R}{Q}(25)}}\frac{v_{probe}(25)}{v_{probe}(n)} \quad . \quad (5)$$

The calculated r/q are shown in Figure 2 together with R/Q and Q_l referred from [1].

The relation between V_{probe}, the beam current (I_b) and the rf source equivalent current (I_{rf}) is written as follows:

$$\frac{d}{dt}\begin{bmatrix}V_r\\V_i\end{bmatrix}=\begin{bmatrix}-\omega_{1/2}(n) & -\Delta\omega(n,t)\\ \Delta\omega(n,t) & -\omega_{1/2}(n)\end{bmatrix}\begin{bmatrix}V_r\\V_i\end{bmatrix}$$
$$+\frac{\omega_0(25)}{2}\frac{R}{Q}(25)\frac{v^2_{probe}(n)}{v^2_{probe}(25)}\left(\begin{bmatrix}I_{rf\_r}\\I_{rf\_i}\end{bmatrix}-\left(\frac{V_{acc}(n)}{V_{probe}(n)}\right)\begin{bmatrix}I_{b\_r}\\I_{b\_i}\end{bmatrix}\right) \quad , \quad (6)$$

$$\omega_{1/2}(n)=\frac{\omega_0(n)}{2Q_l(n)} \quad , \quad (7)$$

$$\Delta\omega(n,t)=\omega_{cav}(n,t)-\omega_{rf}=\omega_{cav}(n,t)-2\pi\cdot 1.3e9 \quad . \quad (8)$$

Here V_r and V_i are the real and imaginary parts of the probe voltage, respectively. Equation (6) means that the beam effect is smaller than that by the rf input.

3 CALCULATION RESULTS

Table 1: Typical parameters for the calculation.

RF pulse	1.6 ms
Beam pulse	1 ms (0.6 ms – 1.6 ms)
Beam	8 nC 1 MHz
R/Q (fundamental)	2998
R/Q (other modes)	10
BPF type	4th Bessel
Loop delay	5 micro s
Feedback gain	50 (34 dB)
Beam acc. set voltage	81 MV [1]
Lorentz force detuning constant	1 (Hz/(MV/m)^2)

A calculation of the system was carried out with the parameters listed in Table 1. The schematic of the system is shown in Figure 3. The beam R/Q are set to 10 to estimate the worst conditions for control. The system stability is examined as function of the BPF bandwidth and analysed by use of Bode plots.

3.1 BPF bandwidth

The results with the parameter of the BPF bandwidth are shown in Figure 4. BPF bandwidth narrower than 150 kHz can sufficiently reduce the 26th mode. The bandwidth narrower than 50 kHz results in a slower response time, leading to poor control. Because the BPF with bandwidth wider than 150 kHz permits excitation of the 26th mode, the fundamental signal is not stable. The 250 kHz down-converter system with optimised BPF enables us to control the fundamental mode.

3.2 Microphonics

In order to analyze the effect of microphonics the feedforward table obtained for a given Lorentz-force detuning curve is also applied for additional +50Hz and -50 Hz detuning as induced by microphonics. Despite the feedforward table mismatch the regulation quality and loop stability do not suffer. The results are summarized in Table 2.

3.3 Bode plot

The system performance is compared with the standard 9-cell cavity system by the Bode plot as shown in Figure 5. Since the 27th mode is located about 370 kHz higher than the fundamental mode, the alias signal (130 kHz) is shown. It is confirmed that the wide-bandwidth BPF (200 kHz) cannot suppress the 26th mode sufficiently and that the narrow-bandwidth BPF (25kHz) results in low gain-margin due to the loop-phase shift.

The gain margin and pseudo-gain margins for the other

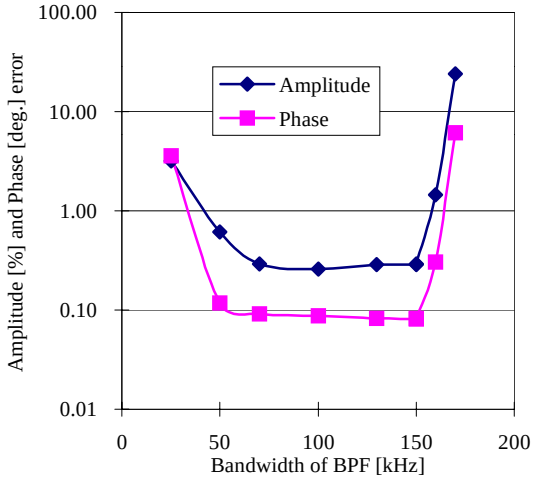

Figure 4 Dependence on the filter bandwidth. The center frequency of the BPF is 250 kHz. The errors become minimum for 50 kHz to 150 kHz bandwidth.

Table 2: Calculation results for mismatched feedforward tables

	Amplitude Error	Phase Error
0 Hz det. by microphonics	0.26%	0.09 deg.
+50 Hz detuning	0.32%	0.09 deg.
–50 Hz detuning	0.27%	0.09 deg.

modes, which are only the difference between 0 dB and peak amplitude without consideration of loop phase, are plotted in Figure 6. Although the real gain margin is different from the pseudo ones, the values are the safety ones because the phase would change due to the system delay. Half of the gain margin represents the gain limit for the feedback operation [2]. The results show that the maximum feedback gain with 70 kHz bandwidth BPF is 38.5 dB. This is about a quarter of the standard TTF control system (=44 dB). However, the gain is still sufficient to reduce the residual errors within the specifications.

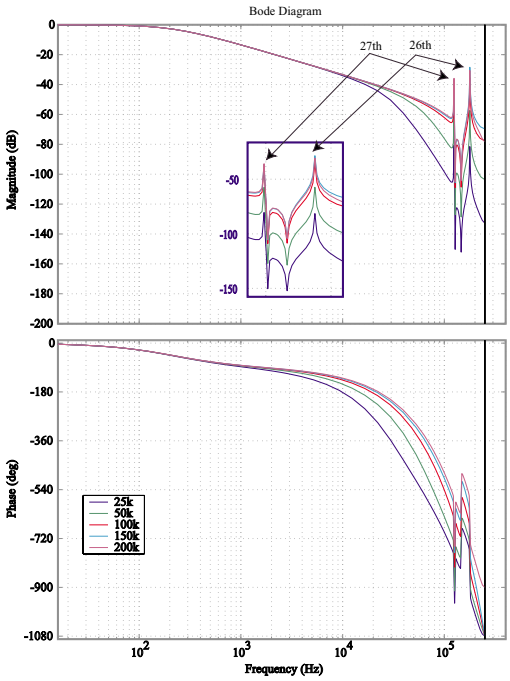

Figure 5 Bode plot for the superstructure cavity with BPF of 25~200 kHz bandwidth. The alias (130 kHz) of the 27th mode located 370 kHz higher than fundamental mode is shown in the figure.

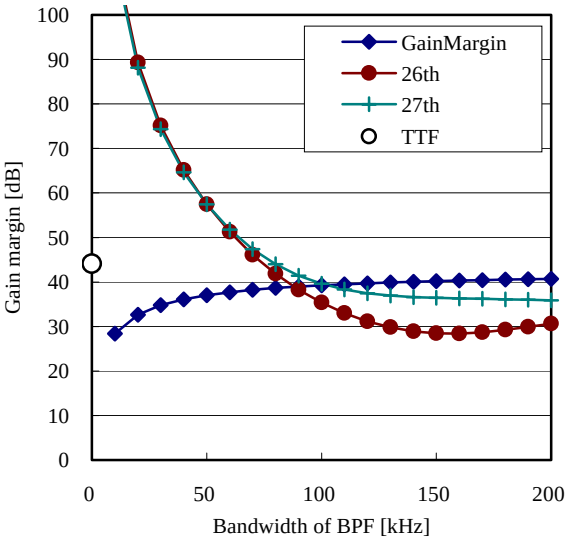

Figure 6 BPF bandwidth dependence on the operational gain. The pseudo-gain margins for the 26th and 27th modes are defined from the gain of the amplitude without considering the phase delay. “TTF” is the gain margin for the p-mode of the standard 9-cell TTF cavity.

5 SUMMARY

The LLRF system presently in operation at the TESLA Test Facility can be used for the superstructure by insertion of a bandpass filter at the IF output of the down converter. The simulation results demonstrate that performance goals are met for a wide range of loop gain and filter bandwidth. A loop gain of 50 and a filter bandwidth of 70 kHz guarantees robustness against parameter variations.

6 REFERENCES

[1] J. Sekutowicz, M. Ferrario, and Ch. Tang, "Superconducting superstructure for the TESLA collider: A concept", Phys. Rev. ST Accel. Beams 2, 062001 (1999).

[2] T.Schilcher, "Vector Sum Control of Pulsed Accelerating Fields in Lorenz Force Detuned Superconducting Cavities", August 1998, TESLA 98-20.

[3] S.N.Simrock, I.Altmann, K.Rehlich, T.Schilcher, “DESIGN OF THE DIGITAL RF CONTROL SYSTEM FOT THE TESLA TEST FACILITY”, EPAC96, Sitges (Barcelona), June 10-14,1996, p.346.